# Structure and energetics of hydrogen clusters. Structures of $H_{11}^+$ and $H_{13}^+$. Vibrational frequencies and infrared intensities of the $H_{2n+1}^+$ clusters ($n=2$–6)

Michel Farizon, Henry Chermette, and Bernadette Farizon-Mazuy
*Institut de Physique Nucléaire de Lyon, IN2P3-CNRS et Université Claude Bernard, 43, Bd du 11 Novembre 1918, F-69622 Villeurbanne Cedex, France*

(Received 15 July 1991; accepted 11 October 1991)

*Ab initio* self-consistent-field (SCF) Hartree–Fock and configuration interaction (CI) calculations have been carried out for $H_{2n+1}^+$ ($n = 1$–6) clusters using a triple-zeta plus polarization basis set. Fully optimized structures and energies of $H_{11}^+$ and $H_{13}^+$ are presented. These structures can be thought as the addition of $H_2$ molecules to a deformed $H_9^+$. Dissociation energies as a function of cluster size follow the pattern established experimentally by Hiraoka and Mori. Nevertheless, our energy results on the biggest clusters suffer from the lack of size consistency of CI with single and double substitutions (CISD) calculations. Analytic gradient techniques have been used to locate stationary point geometries and to predict harmonic vibrational frequencies and infrared intensities at the two levels of theory SCF ($n = 1$–6) and CISD ($n = 1$–4) both with triple-zeta plus polarization basis sets. Of special interest are the new vibrational modes of $H_{11}^+$ and $H_{13}^+$, which have no counterpart in the $H_9^+$ cluster. Our predicted frequencies compare fairly well with the experimental results of Okumura, Yeh, and Lee.

## I. INTRODUCTION

Positive hydrogen cluster ions are of considerable theoretical[1–6] and experimental interest[7–16] since they are perhaps the simplest example of molecular clustering. The $H_5^+$ ion was first identified positively by Dawson and Tickner in 1962[10] by mass spectrometry. Larger odd mass clusters were observed subsequently by Buckheit and Henkes[7] in mass spectra and by Clampit and Gowland[8] using low energy electron bombardement of solid hydrogen. Later workers have observed odd mass hydrogen clusters in various size distributions from ionization and collisional fragmentation studies. Kirchner and Bowers[10] have studied the dynamics of metastable $H_5^+$ fragmentation. Directly pertinent to the present theoretical study are experimental measurements[12,13] of the dissociation energies for the processes

$$H_3^+(H_2)_{n-2} + H_2 \cdots H_3^+(H_2)_{n-1}.$$

The most recent measurements of Hiraoka and Mori[13] (HM) give thermochemical data for $-\Delta H^0_{n-2,n-1}$ and $-\Delta S^0_{n-2,n-1}$ with $n = 1$–10. From a chemical perspective, the most important experimental paper to date is the one written by Okumura, Yeh, and Lee[15] (OYL) of the infrared absorption frequencies. From vibrational predissociation spectroscopy, OYL have measured the vibrational spectra of the cluster $H_{2n+1}^+$ with $n = 1$–6 which were observed near 4000 $cm^{-1}$. From Coulomb explosion experiments,[16] the interaction of hydrogen clusters with matter has been studied.

There have been a substantial number of theoretical studies of positive hydrogen clusters with the most recent and reliable investigation being that of Yamaguchi, Gaw, Remington, and Schaefer[5] (YGRS) for the $H_5^+$ species. Moving to the larger $H_{2n+1}^+$ species, at least three systematic studies of $H_7^+$ and $H_9^+$ [2,5,6] and in the two cases of $H_{11}^+$ and $H_{13}^+$ [2,3] have been reported at both the self-consistent field (SCF) and configuration interaction including all single and double excitations (CISD) level of theory. Another study of Huber[3] has given near-Hartree–Fock energies and structures of $H_{2n+1}^+$ ($n = 1$–6) applying the floating orbital geometry optimization (FOGO). The study of YGRS[5] predicts harmonic vibrational frequencies for $H_7^+$ and $H_9^+$ with a double-zeta plus polarization basis set. To our knowledge, the present report represents the first theoretical predictions of the vibrational frequencies and infrared intensities of $H_{11}^+$ and $H_{13}^+$.

## II. THEORETICAL APPROACH

In our previous theoretical study,[6] *ab initio* SCF and configuration interaction (CI) calculations have been carried out for $H_{2n+1}^+$ ($n = 1$–4) clusters with a triple-zeta plus polarization basis set. In the present report, the research of Ref. 6 has been extended simultaneously in several directions. First, the two clusters $H_{11}^+$ and $H_{13}^+$ have been considered at both levels of theory adopted triple-zeta plus polarization (TZP) SCF and TZP CISD. The precise TZP basis set was the Pople set with five primitive *s* functions, contracted to three *s* functions, and *p* functions with the orbital exponent 0.75. This basis set is not complete. Nevertheless, in our previous paper, we have shown the accuracy of this basis set by comparing SCF energies for our most stable structures of $H_3^+$ and $H_5^+$ with the best value in the literature. With the same basis set, correlation effects were considered variation-

ally by means of CISD. The CISD method is well known to suffer from the absence of size consistency. To take into account this problem, the size consistency corrections (SCC) have been estimated according to Davidson's scheme, as in our previous paper. Full geometry optimizations have been done, the optimization being stopped when the magnitude of the gradient is below $10^{-5}$ a.u. Moreover since some of these potential hypersurfaces are extremely flat in the region of the stationnary points, a harmonic vibrational analysis may be required to ascertain the character of each stationnary point (local minimum or saddle point). Analytic SCF and CI gradient methods were used to locate the stationary point geometries and analytic force constants were calculated to evaluate harmonic vibrational frequencies. All computations, performed with Gaussian-86 programs, were carried out on the IBM 3090 of the computer center of the IN2P3 at Villeurbanne ($F$).

## III. THE $H_{11}^+$ AND $H_{13}^+$ CLUSTER IONS

### A. Structures

Among theoretical studies of $H_{11}^+$, the work of Huber[3] is the only one giving a full geometry optimized structure, the optimization being stopped when the magnitude of the gradient is below 0.001 a.u. However, a harmonic vibration analysis of this structure exhibits imaginary frequencies; consequently, it is not a minimum. The fully optimized geometry of $H_{11}^+$, predicted at both levels of theory TZP SCF and TZP CISD, is shown in Fig. 1 with symmetry assignment $C_s$. The optimized structures and their predicted energies are compiled in Table I. The structure can be thought as the addition of a $H_2$ molecule to a $H_9^+$ unit (where the $H_2$ subunits lie perpendicularly to the $H_3^+$ plane). The $H_2$ molecule is added parallel to the $H_3^+$ plane, but perpendicular to one of the H–H axis of the $H_3^+$ core. Nevertheless, all the parameters being free during the optimization, a weak deformation of the $H_9^+$ core is observed and, unlike previous reports, the additional $H_2$ is found to be off center with respect to the center of the $H_3^+$ core by more than 16 pm. The geometrical parameters most sensitive to the level of theory are the distances between the $H_2$ midpoints and the nearest protons of the $H_3^+$ core. Electron correlation reduces this $H_3^+ \cdots H_2$ separation by more than 10 pm. The distance between the additional $H_2$ and the deformed $H_9^+$ core is also reduced from TZP SCF to TZP CISD levels by more than 10 pm. However, the distances in the $H_3^+$ increase from 87.51 to 88.74 and from 87.74 to 89.04 pm.

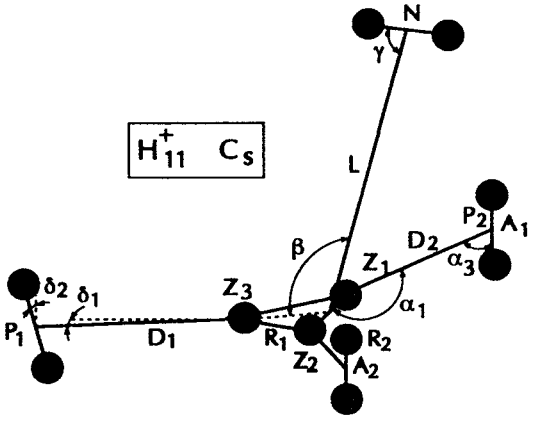


FIG. 1. The structure of $H_{11}^+$.

On the basis of the results presented here for $H_{11}^+$, it is reasonable to assume for $H_{13}^+$ a $C_{2v}$ structure of the type seen in Fig. 2 which presents our fully optimized geometrical predictions. The optimized structures and their energies are compiled in Table II. This $C_{2v}$ structure places each of the two $H_2$ subunits in opposite positions with respect to the $H_3^+$ plane, parallel to this plane, but off center. The same trend as in $H_{11}^+$ is seen concerning the theoretical values of the distance from the three equivalent H atoms of the $H_3^+$ core to the bond midpoint of the nearest $H_2$ molecule—176.75 pm (TZP SCF) and 165.17 pm (TZP CISD), for example. The electron correlation reduces these $H_3^+ \cdots H_2$ separation by more than 11 pm. This trend is also seen for the $H_9^+ \cdots H_2$ distance.

Furthermore, on the basis of our previous theoretical studies and the results presented here for $H_{11}^+$ and $H_{13}^+$, some typical distances which are representative of the $H_3^+ \cdots H_2$ interaction ($D$), the $H_9^+ \cdots H_2$ interaction ($L$), the $H_3^+$ core ($R$), and the $H_2$ subunits ($P$ and $N$) are reported in Table III at both levels of theory (TZP SCF and TZP CISD). Since from $H_9^+$ the three $H_2$ ligands share equal attraction provided by the central positive charge, each $H_3^+ \cdots H_2$ interaction is necessarily weaker. This fact is reflected first in the distances $D$ between the nearest proton of the $H_3^+$ core and the midpoints of $H_2$ subunits. At both SCF and CI levels of theory, these distances $D$ increase with the mass number $n$ until reaching a nearly constant value ($\sim 177$ pm at the SCF level and $\sim 167$ pm at the CI level) for $n$ greater than 7. Similarly, the distance $L$ between each added $H_2$ subunit and the deformed $H_9^+$ core, about 290 pm, is changed by less than 4 pm from $H_{11}^+$ to $H_{13}^+$. Furthermore, due to the deformation of the $H_9^+$ core, there are two H–H distances in the central $H_3^+$ core. Comparing these distances with the analogous distance in $H_9^+$, one observes that the $H_{13}^+$ cluster is more deformed than the $H_{11}^+$ cluster. Specifically, at the TZP SCF level, for $H_{13}^+$ the distances $R$ are 87.38 and 87.84 pm when for $H_{11}^+$ the analogous distances are 87.51 and 87.74 pm. The same trend is seen at the CISD level. Finally, at both levels of theory, the distances $P$ in the $H_2$ subunits of the $H_9^+$ core decrease with $n$ and tend to reach a nearly constant value (74.28 pm for $H_{11}^+$ and 74.26 pm for $H_{13}^+$ at the SCF level) closer to the H–H distance in isolated molecular hydrogen (73.55 pm at the SCF level). Furthermore, at the SCF level, the distances $N$ (73.70 pm) in the added $H_2$ subunits for $H_{11}^+$ and $H_{13}^+$ are still smaller than the distances $P$ in the other $H_2$ subunits and, of course, closer to the 73.55 pm value. Nevertheless, at the CISD level, these distances $N$ (74.24 and 74.18 pm for $H_{11}^+$ and $H_{13}^+$, respectively) get on values smaller than the distance in isolated molecular hydrogen (74.39 at the CISD level). It must be noted that the CI including single and double excitations represents an exact

TABLE I. Energies and structures of $H_{11}^+$ at TZP SCF and TZP CISD levels of theory. $\alpha_2$ is the angle between the $H_3^+$ nucleus plane ($Z_1 Z_2 Z_3$) and the $A_1 Z_1 Z_2 A_2$ plane. Other symbols are indicated in Fig. 1.

| Level of theory | Energy (a.u.) | ZPE (a.u.) | SCC (a.u.) | $R_1$ (pm) | $R_2$ (pm) | $D_1$ (pm) | $D_2$ (pm) | $P_1$ (pm) | $P_2$ (pm) | $\alpha_1$ (degree) | $\alpha_2$ (degree) | $\alpha_3$ (degree) | $\delta_1$ (degree) | $\delta_2$ (degree) | $L$ (pm) | $\beta$ (degree) | $\gamma$ (degree) | $N$ (pm) |
|---|---|---|---|---|---|---|---|---|---|---|---|---|---|---|---|---|---|---|
| SCF | −5.847 082 | 0.076 385 | | 87.51 | 87.74 | 177.88 | 176.95 | 74.28 | 74.28 | 174.11 | 84.11 | 87.79 | 0.25 | 0.05 | 286.34 | 88.87 | 112.42 | 73.70 |
| CISD | −6.024 303 | | −0.011 376 | 88.74 | 89.04 | 167.28 | 165.56 | 74.96 | 74.96 | 174.46 | 84.46 | 88.03 | 0.20 | 0.06 | 273.58 | 88.72 | 112.56 | 74.24 |

solution of the correlation problem for $H_2$ and $H_3^+$. For $H_{2n+1}^+$, there are at least additional errors inherent in the CISD wave functions due to their neglect of true many-body correlation effects, i.e., triple, quadruple, and higher excitations relative to the Hartree–Fock reference configuration.

### B. Energetics

As in our previous work,[6] we present in Table IV dissociation energies $D_e$ for the abstraction of molecular hydrogen from $H_{2n+1}^+$ with $n = 5$–6 at TZP SCF and TZP CISD levels of theory. The dissociation energies $D_0$ are obtained by taking into account zero-point vibrational energies of reactants and products. This correction has been done within the harmonic approximation. The predicted dissociation energies $D_e$ exhibit the experimental trend as a function of the cluster size established by several authors. The energies required to remove molecular hydrogen from $H_5^+$, $H_7^+$, $H_9^+$, $H_{11}^+$, and $H_{13}^+$ are 32.77, 15.44, 13.8, 4.02, and 3.72 kJ, respectively, at the highest level of theory, compared to the HM experimental values 29.80, 14.56, 14.02, 7.70, and 7.57 kJ (see also our previous work[6]). Nevertheless, a relatively poor agreement is obtained at the CISD level for $H_{11}^+$ and $H_{13}^+$ probably due to the size consistency error problem, the magnitude of SCC growing rapidly with the cluster size. However, one can notice the gap between the stabilities of the $H_5^+$–$H_7^+$–$H_9^+$ group and the $H_{11}^+$–$H_{13}^+$ group. Furthermore, the predicted dissociation energies $D_0$ show that within the harmonic approximation, there is a large correction to the dissociation energy due to zero-point vibrational energy, namely about 12.5 kJ. The addition of zero-point energy (ZPE) effects significantly worsens the agreement between theory and experiment. The strong anharmonicity of the vibrations of these clusters is probably responsible of a part of such a behavior.

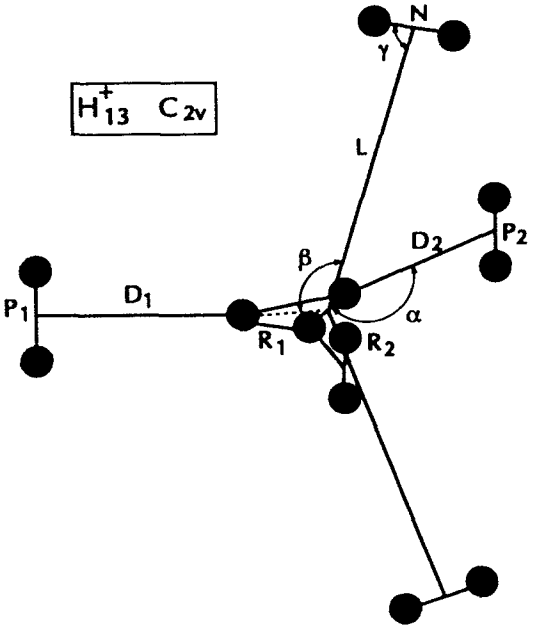


FIG. 2. The structure of $H_{13}^+$.

## IV. VIBRATIONAL FREQUENCIES

For all $H_{2n+1}^+$ clusters, harmonic vibrational frequencies were predicted at the TZP SCF level of theory and until $n$ equal 9 at the TZP CISD level of theory. These results are shown in Tables V and VI. The first significant point is that all the structures are true minima.

The comparison between TZP SCF and TZP CISD vibration frequencies illustrates the importance of the correlation effects. For $H_5^+$, the correlation effects reduce the highest frequency [$H_2$ stretch ($A_1$)] by (4397–4140) = 257 $cm^{-1}$. Also decreasing with the inclusion of correlation are the $H_3^+$ asymmetric stretch ($B_2$) by 484 $cm^{-1}$ and the $H_3^+$ symmetric stretch ($A_1$) by 628 $cm^{-1}$. In contrast, the $H_3^+$ symmetric stretch ($A_1$) increases by less than 90 $cm^{-1}$ in going from SCF to CISD. The modes not present in infinitely separated $H_3^+ + H_2$ are also increasing with the inclusion of the correlation: the highest frequency is the $B_1$ mode ($H_3^+$ wag + $H_2$ rock) at 1253 $cm^{-1}$ (CISD level) and the lowest is the $A_2$ mode (torsional motion about the hydrogen-bonded distance $R$) at 214 $cm^{-1}$ (CISD level). As the most reliable previous report of YGRS,[5] one can conclude that for this weakly bound system, the effects of correlation on the predicted vibrational frequencies do not fall into a simple pattern.

In the $H_7^+$ case, one can see from Tables V and VI that all five highest vibrational frequencies above 2000 $cm^{-1}$ are reduced by the electron correlation effect. From SCF to CISD, these reductions are 161, 162, 131, 162, and 282 $cm^{-1}$. The five $H_7^+$ frequencies under consideration here correspond to those arising from infinitely separated $H_3^+ + H_2 + H_2$. Among the other high frequency normal modes, the two highest frequencies (CISD level) at 4304 and 4299 $cm^{-1}$ are split by only 5 $cm^{-1}$ and lie at 110 and

TABLE II. Energies and structures of $H_{13}^+$ at TZP SCF and TZP CISD levels of theory. Symbols are indicated in Fig. 2.

| Level of theory | Energy (a.u.) | ZPE (a.u.) | SCC (a.u.) | $R_1$ (pm) | $R_2$ (pm) | $D_1$ (pm) | $D_2$ (pm) | $P_1$ (pm) | $P_2$ (pm) | $\alpha$ (degree) | $L$ (pm) | $\beta$ (degree) | $\gamma$ (degree) | $N$ (pm) |
|---|---|---|---|---|---|---|---|---|---|---|---|---|---|---|
| SCF | −6.980 708 | 0.088 384 | | 87.38 | 87.84 | 178.75 | 176.74 | 74.26 | 74.26 | 153.02 | 289.42 | 109.30 | 89.02 | 73.70 |
| CISD | −7.189 196 | | −0.016 283 | 88.46 | 89.20 | 168.52 | 165.17 | 74.88 | 74.90 | 152.24 | 275.08 | 109.68 | 88.84 | 74.18 |

105 $cm^{-1}$, respectively, below the harmonic frequency predicted for the isolated $H_2$ molecule. Electron correlation has a significant effect on the next vibrational frequencies, i.e., those ranging from 993 to 126 $cm^{-1}$. All of these frequencies are increased in going from SCF to CISD. Nevertheless, the two lowest vibrational frequencies which are internal rotations are not very sensitive to correlation effects. They are increased by less than 24 $cm^{-1}$ from the SCF to the CISD level.

In the $H_9^+$ case, among the 21 vibrational degrees of freedom, there are seven doubly degenerate frequencies and an equal number of nondegenerate frequencies. From these 14 distinct frequencies, only four correspond to those arising from infinitely separated $H_3^+ + H_2 + H_2 + H_2$. The same trend as in the $H_7^+$ case is obtained concerning the electron correlation effects on the vibrational frequencies.

In the $H_{11}^+$ and $H_{13}^+$ cases, we did not perform vibrational frequencies at the CISD level due to computer time and space memory. Nevertheless, our SCF results exhibit nearly the same vibrational frequencies as in $H_9^+$, due to the weak deformation of the $H_9^+$ core by approaching one or two $H_2$ ligands. Concerning the "new" modes of $H_{11}^+$, the most interesting mode is the highest frequency at 4572 $cm^{-1}$ of the added $H_2$. Due to the weak $H_9^+ \cdots H_2$ interaction, this vibrational frequency is below the harmonic frequency predicted for the isolated molecule by less than 21 $cm^{-1}$. Concerning the new modes of $H_{13}^+$, the two highest frequencies correspond to the two additional $H_2$. These frequencies at 4573 $cm^{-1}$ are equal to those of $H_{11}^+$.

Since $H_{2n+1}^+$ may be described qualitatively as $H_3^+ (H_2)_n$, it is appropriate to compare the highest frequencies with those of $H_2$ and $H_3^+$. Turning first to the variation of the $H_2$ stretching frequency lying close to the $H_3^+$ core with the cluster size, it is seen that this frequency increases with the cluster size until reaching a value below the harmonic frequency predicted for the isolated molecule (4594) by less than 100 $cm^{-1}$. These frequencies are 4397; 4461 and 4465; 4487 (degenerate) and 4492; 4489, 4490, and 4495; 4492, 4492, and 4497 $cm^{-1}$ for $H_5^+$, $H_7^+$, $H_9^+$, $H_{11}^+$, and $H_{13}^+$, respectively. Let us notice that for bigger clusters than $H_9^+$, the frequencies change by less than 10 $cm^{-1}$ with the cluster size. That is not surprising due to the weak deformation of the core $H_9^+$ in these clusters. Turning to the variation of the symmetric stretching frequency of $H_3^+$ with the cluster size, these frequencies are always found below the equivalent harmonic frequency predicted for the isolated

TABLE III. Typical bond lengths of the optimized geometries of $H_{2n+1}^+$ ($n = 1$–6) at both levels of theory TZP SCF and TZP CISD. Symbols are indicated in the text.

| | $H_2$ | $H_3^+$ | $H_5^+$ | $H_7^+$ | $H_9^+$ | $H_{11}^+$ | $H_{13}^+$ |
|---|---|---|---|---|---|---|---|
| TZP SCF | | | | | | | |
| $D$ (pm) | | | 149.07 | 167.64 | 177.01 | 177.88 | 178.75 |
| | | | | | | 176.95 | 176.71 |
| TZP CISD | | | | | | | |
| $D$ (pm) | | | 125.46 | 155.19 | 165.80 | 167.28 | 168.52 |
| | | | | | | 165.56 | 165.17 |
| TZP SCF | | | | | | | |
| $R$ (pm) | | 86.95 | 82.69 | 86.32 | 87.66 | 87.51 | 87.38 |
| | | | 91.91 | 91.51 | | 87.74 | 87.84 |
| TZP CISD | | | | | | | |
| $R$ (pm) | | 87.80 | 81.01 | 87.23 | 89.01 | 88.74 | 88.46 |
| | | | 99.51 | 94.92 | | 89.04 | 89.20 |
| TZP SCF | | | | | | | |
| $P$ (pm) | 73.55 | | 75.06 | 74.50 | 74.38 | 74.28 | 74.26 |
| | | | | | | 74.28 | 74.26 |
| TZP CISD | | | | | | | |
| $P$ (pm) | 74.39 | | 76.85 | 75.44 | 75.02 | 74.96 | 74.89 |
| | | | | | | 74.94 | 74.89 |
| TZP SCF | | | | | | | |
| $N$ (pm) | | | | | | 73.70 | 73.70 |
| TZP CISD | | | | | | | |
| $N$ (pm) | | | | | | 74.24 | 74.18 |

TABLE IV. Theoretical and experimental values of dissociation energies of $H_{2n+1}^+$ ($n = 5,6$) at TZP SCF and TZP CISD levels of theory (SCC included). Calculations are performed using those described in Ref. 6.

| $H_{2n+1}^+$ | $D_e^{SCF}$ (kJ) | $D_0^{SCF}$ (kJ) | $D_e^{CISD}$ (kJ) | $-\Delta H$(expt.) (kJ) |
|---|---|---|---|---|
| $H_{11}^+$ | 3.10 | −1.30 | 4.02 | $7.70 \pm 0.2$[a] |
| $H_{13}^+$ | 2.97 | −1.04 | 3.72 | $7.57 \pm 0.2$[a] |

[a] Reference 13.

molecule (3538 $cm^{-1}$), except for $H_5^+$. These frequencies are 3647, 3457, 3406, 3415, and 3423 $cm^{-1}$ for $H_5^+$, $H_7^+$, $H_9^+$, $H_{11}^+$, and $H_{13}^+$, respectively. Likewise, the $H_3^+$ degenerate bending frequency (2859 $cm^{-1}$) is reduced in larger clusters by 333 and 482; 166 and 346; 203 (degenerate); 188 and 202; 175 and 205 $cm^{-1}$ for $H_5^+$, $H_7^+$, $H_9^+$, $H_{11}^+$, and $H_{13}^+$, respectively.

In Table VII are gathered selected experimental results from OYL, theoretical results from YGRS, and this work. The comparison concerns the $H_2$ stretching frequency related to the $H_2$ subunits lying close to the $H_3^+$ core (i.e., limited to the three $H_2$ of the $H_9^+$ core in case of bigger clusters). Turning first at the TZP SCF level to the $H_2$ stretching frequency, one notes that for the isolated $H_2$ molecule the TZP SCF harmonic frequency (4594 $cm^{-1}$) is 433 $cm^{-1}$ higher than the observed (anharmonic) fundamental (4161 $cm^{-1}$).[17] Substracting this same 433 $cm^{-1}$ from the analogous $H_{2n+1}^+$ harmonic frequency yields the prediction $\nu$ (H–H) = 3964; 4032 and 4036; 4059 and 4054 (degenerate); 4062, 4057, and 4056; 4064 and 4059 (degenerate) $cm^{-1}$ for $H_5^+$, $H_7^+$, $H_9^+$, $H_{11}^+$, and $H_{13}^+$; respectively. These results must be compared to the experimental frequencies of OYL 3910, 3980, 4020, 4028, and 4035 $cm^{-1}$ for $H_5^+$, $H_7^+$, $H_9^+$, $H_{11}^+$, and $H_{13}^+$, respectively. Then, the experimental frequencies lie at 54; 52 and 56; 39 and 34; 34, 29, and 28; 29 and 24 $cm^{-1}$ for $H_5^+$, $H_7^+$, $H_9^+$, $H_{11}^+$, and $H_{13}^+$, respectively, above the present predictions. One notes that the agreement increases with the cluster size. One concludes that the $H_3^+ \cdots H_2$ picture describes more precisely the collective bonding in $H_{13}^+$ than in $H_5^+$, for example. YGRS had already noted in their study of $H_5^+$ that these scaling procedures are somewhat unreliable for this system, even with a large basis set at the full CI level. We have to note that with this scaling procedure on the DZP SCF results of YGRS, OYL found a better agreement than with the present predictions at the TZP SCF level. Nevertheless, OYL found a poorer agreement when they compared their experimental results with the best calculations of YGRS. Using the same scaling pro-

TABLE V. Harmonic vibrational frequencies (in $cm^{-1}$) for $H_2$ and $H_{2n+1}^+$ ($n = 1$–6) at the TZP SCF level of theory.

| | $H_2$ | $H_3^+$ | | $H_5^+$ | | $H_7^+$ | | $H_9^+$ | | $H_{11}^+$ | | $H_{13}^+$ | |
|---|---|---|---|---|---|---|---|---|---|---|---|---|---|
| 1 | | | | | | | | | | | | 26 | (A 1) |
| 2 | | | | | | | | 48 | (A 1″) | 38 | (A′) | 41 | (B 2) |
| 3 | | | | | | | | 75 | (E″) | 60 | (A″) | 56 | (A 2) |
| 4 | | | | | | 102 | (A 2) | 75 | (E″) | 79 | (A″) | 78 | (B 1) |
| 5 | | | | | | | | 111 | (E′) | 102 | (A″) | 86 | (A 2) |
| 6 | | | | | | 117 | (B 1) | 111 | (E′) | 111 | (A″) | 109 | (B 1) |
| 7 | | | | | | | | | | 112 | (A′) | 113 | (A 2) |
| 8 | | | | | | | | | | 119 | (A′) | 120 | (A 1) |
| 9 | | | | | | | | | | | | 131 | (A 1) |
| 10 | | | | | | | | | | | | 136 | (B 2) |
| 11 | | | | | | | | | | 142 | (A′) | 138 | (B 1) |
| 12 | | | | | | | | | | 149 | (A″) | 148 | (B 2) |
| 13 | | | | | | | | | | | | 162 | (A 2) |
| 14 | | | | 181 | (A 2) | 159 | (A 1) | 185 | (A 2″) | 191 | (A′) | 199 | (B 2) |
| 15 | | | | | | | | | | 299 | (A″) | 290 | (A 1) |
| 16 | | | | | | | | | | | | 291 | (B 2) |
| 17 | | | | | | 378 | (B 2) | 376 | (A 1′) | 373 | (A′) | 370 | (B 1) |
| 18 | | | | | | | | 382 | (E′) | 373 | (A″) | 370 | (A 1) |
| 19 | | | | | | 481 | (A 1) | 382 | (E′) | 385 | (A′) | 387 | (A 1) |
| 20 | | | | 526 | (A 1) | 540 | (B 1) | 624 | (E″) | 612 | (A″) | 601 | (A 2) |
| 21 | | | | | | | | 624 | (E″) | 614 | (A′) | 602 | (B 2) |
| 22 | | | | 678 | (B 2) | 685 | (B 1) | 693 | (A 2″) | 694 | (A′) | 696 | (B 2) |
| 23 | | | | | | 699 | (B 2) | 724 | (A 2′) | 717 | (A″) | 715 | (B 1) |
| 24 | | | | 781 | (B 1) | 779 | (B 1) | 802 | (E″) | 785 | (A′) | 768 | (B 2) |
| 25 | | | | 1012 | (B 1) | 888 | (A 2) | 802 | (E″) | 787 | (A″) | 775 | (A 2) |
| 26 | | 2859 | (E′) | 2377 | (A 1) | 2513 | (A 1) | 2656 | (E′) | 2657 | (A′) | 2654 | (A 1) |
| 27 | | 2859 | (E′) | 2526 | (B 2) | 2693 | (B 2) | 2656 | (E′) | 2671 | (A″) | 2684 | (B 1) |
| 28 | | 3538 | (A 1′) | 3647 | (A 1) | 3457 | (A 1) | 3406 | (A 1′) | 3415 | (A′) | 3423 | (A 1) |
| 29 | | | | | | 4461 | (B 2) | 4487 | (E′) | 4489 | (A′) | 4492 | (A 1) |
| 30 | | | | 4397 | (A 1) | 4465 | (A 1) | 4487 | (E′) | 4490 | (A″) | 4492 | (B 1) |
| 31 | | | | | | | | 4492 | (A 1′) | 4495 | (A′) | 4497 | (A 1) |
| 32 | | | | | | | | | | 4572 | (A′) | 4573 | (B 2) |
| 33 | 4594 | | | | | | | | | | | 4573 | (A 1) |

TABLE VI. Harmonic vibrational frequencies (in $cm^{-1}$) for $H_2$ and $H_{2n+1}^+$ ($n = 1$–4) at the TZP CISD level of theory.

| | $H_2$ | $H_3^+$ | | $H_5^+$ | | $H_7^+$ | | $H_9^+$ | |
|---|---|---|---|---|---|---|---|---|---|
| 1 | | | | | | | | 67 | ($A1''$) |
| 2 | | | | | | | | 86 | ($E''$) |
| 3 | | | | | | 116 | ($A2$) | 86 | ($E''$) |
| 4 | | | | | | | | 135 | ($E'$) |
| 5 | | | | | | 129 | ($B1$) | 135 | ($E'$) |
| 6 | | | | 214 | ($A2$) | 199 | ($A1$) | 219 | ($A2''$) |
| 7 | | | | | | | | 444 | ($E'$) |
| 8 | | | | | | 411 | ($B2$) | 444 | ($E'$) |
| 9 | | | | 511 | ($A1$) | 596 | ($A1$) | 458 | ($A1'$) |
| 10 | | | | | | | | 656 | ($E''$) |
| 11 | | | | | | 629 | ($B1$) | 656 | ($E''$) |
| 12 | | | | | | 731 | ($B1$) | 711 | ($A2''$) |
| 13 | | | | 891 | ($B2$) | 827 | ($B2$) | 845 | ($A2'$) |
| 14 | | | | 921 | ($B1$) | 828 | ($B1$) | 894 | ($E''$) |
| 15 | | | | 1253 | ($B1$) | 993 | ($A2$) | 894 | ($E''$) |
| 16 | | 2746 | ($E'$) | 1749 | ($A1$) | 2231 | ($A1$) | 2477 | ($E'$) |
| 17 | | 2746 | ($E'$) | 2042 | ($B2$) | 2531 | ($B2$) | 2477 | ($E'$) |
| 18 | | 3454 | ($A1'$) | 3731 | ($A1$) | 3326 | ($A1$) | 3265 | ($A1''$) |
| 19 | | | | | | | | 4347 | ($E'$) |
| 20 | | | | | | 4299 | ($B2$) | 4347 | ($E'$) |
| 21 | 4414 | | | 4140 | ($A1$) | 4304 | ($A1$) | 4355 | ($A1'$) |

cedure, our predictions at the TZP CISD level are 3887; 4051 and 4046; 4094 and 4102 $cm^{-1}$ for $H_5^+$, $H_7^+$, and $H_9^+$, respectively. Even though at the SCF level the trend of the predicted frequencies is in good agreement with the trend of the experimental values, this is not true at the CISD level. This can be due to the neglect of higher excitations. YGRS have shown the importance of triple and quadruple excitations when they compare their DZP CISD and DZP full CI vibrational frequencies on $H_5^+$.

Turning now to the $H_3^+$ symmetric stretching frequen-

TABLE VII. Some theoretical harmonic vibrational frequencies (in $cm^{-1}$) for $H_2$ and $H_{2n+1}^+$ ($n = 2$–6) at TZP SCF and TZP CISD levels of theory, OYL experimental results (Ref. 15) and YGRS (Ref. 5) theoretical results.

| | $H_2$ | $H_5^+$ | $H_7^+$ | $H_9^+$ | $H_{11}^+$ | $H_{13}^+$ |
|---|---|---|---|---|---|---|
| This work | | | | | | |
| TZP SCF | | | | | | |
| $H_2$ $\nu$(H–H) ($cm^{-1}$) | 4594 | 4397 | 4465 | 4492 | 4495 | 4497 |
| | | | 4461 | 4487 | 4490 | 4492 |
| | | | | 4487 | 4489 | 4492 |
| This work | | | | | | |
| TZP CISD | | | | | | |
| $H_2$ $\nu$(H–H) ($cm^{-1}$) | 4414 | 4140 | 4304 | 4355 | | |
| | | | 4299 | 4347 | | |
| | | | | 4347 | | |
| YGRS | | | | | | |
| DZP SCF | | | | | | |
| $H_2$ $\nu$(H–H) ($cm^{-1}$) | 4657 | 4434 | 4491 | 4516 | | |
| | | | | 4516 | | |
| YGRS | | | | | | |
| DZP CISD | | | | | | |
| $H_2$ $\nu$(H–H) ($cm^{-1}$) | 4533 | 4235 | 4380 | | | |
| | | | 4380 | | | |
| YGRS | | | | | | |
| DZP full CI | | | | | | |
| $H_2$ $\nu$(H–H) ($cm^{-1}$) | 4515 | 4198 | | | | |
| Experiment | | | | | | |
| $H_2$ $\nu$(H–H) ($cm^{-1}$) | 4161[a] (Anharmonic) 4401[a] (Harmonic) | 3910[b] | 3980[b] | 4020[b] | 4028[b] | 4035[b] |

[a] Reference 17.
[b] Reference 15.

cy at the TZP SCF level of theory, one notes that for the isolated $H_3^+$ molecule the harmonic frequency (3538 $cm^{-1}$) is 363 $cm^{-1}$ higher than the latest theoretical prediction (3175 $cm^{-1}$). Substracting this same 363 $cm^{-1}$ from the analogous $H_{2n+1}^+$ harmonic frequency yields the prediction $\nu(A_1) = 3284$, 3094, 3043, 3052, and 3060 $cm^{-1}$ for $H_5^+$, $H_7^+$, $H_9^+$, $H_{11}^+$, and $H_{13}^+$, respectively. Only the analogous true fundamental frequency of $H_5^+$ has been measured by OYL [$\nu(A_1) = 3532$ $cm^{-1}$]. This poor agreement specific to the $H_5^+$ case as seen above should be better with the biggest clusters studied here.

The degenerate asymmetric stretching frequency of $H_3^+$ has been observed by Oka[14] at 2522 $cm^{-1}$. We can use this information to estimate the analogous hydrogen stretches in $H_{2n+1}^+$. This is done by noting that Oka's $\nu(E)$ for $H_3^+$ lies 347 $cm^{-1}$ below the TZP SCF harmonic vibrational frequency. Thus, we estimate the fundamental frequencies 2179 and 2030; 2346 and 2166; 2309 (degenerate); 2324 and 2310; 2337 and 2307 $cm^{-1}$ for $H_5^+$, $H_7^+$, $H_9^+$, $H_{11}^+$, and $H_{13}^+$, respectively. Using the same procedure at the CISD level, we estimate the fundamental frequencies 1817 and 1525; 2306 and 2007; 2254 (degenerate); 2324 and 2310; 2337 and 2307 $cm^{-1}$ for $H_5^+$, $H_7^+$, and $H_9^+$, respectively. One notes that these frequencies lie not very far from the $H_3^+$ fundamental, $H_5^+$ excepted.

Turning to the outer $H_2$ molecules added in the $H_{11}^+$ and $H_{13}^+$ clusters, we can also estimate the fundamental frequencies by a scaling procedure. Indeed, one notes that for the isolated $H_2$ molecule, the TZP SCF harmonic frequency (4594 $cm^{-1}$) is 433 $cm^{-1}$ higher than the observed (anharmonic) fundamental (4161 $cm^{-1}$). Substracting this same 433 $cm^{-1}$ from the highest harmonic frequencies of $H_{11}^+$ and $H_{13}^+$ clusters yields the prediction 4139 and 4140 $cm^{-1}$ for $H_{11}^+$ and $H_{13}^+$, respectively. These predictions must be compared to the weak shoulders observed near 4080–4100 $cm^{-1}$ in clusters larger than $H_9^+$ which is certainly due to the absorption by these outer $H_2$. One notes that the difference observed between experiment and theoretical results is greater than in the case of the three $H_2$ bonds to the three apexes of the $H_3^+$ ion.

## V. INFRARED INTENSITIES

Table VIII presents IR intensities at the TZP SCF level for the $H_{2n+1}^+$ ($n = 1$–6) minima. Since no theoretical infrared intensities have been predicted previously for $H_{2n+1}^+$

TABLE VIII. Infrared intensities (in km/mol) for $H_2$ and the $H_{2n+1}^+$ ($n = 1$–6) at the TZP SCF level of theory.

| | $H_2$ | $H_3^+$ | $H_5^+$ | $H_7^+$ | $H_9^+$ | $H_{11}^+$ | $H_{13}^+$ |
|---|---|---|---|---|---|---|---|
| 1 | | | | | | | 17.53 |
| 2 | | | | | 0 | 8.31 | 3.13 |
| 3 | | | | | 0 | 0.12 | 0 |
| 4 | | | | 0 | 0 | 3.84 | 21.99 |
| 5 | | | | | 7.80 | 8.07 | 0 |
| 6 | | | | 11.78 | 7.80 | 6.99 | 11.67 |
| 7 | | | | | | 1.40 | 0 |
| 8 | | | | | | 10.20 | 13.89 |
| 9 | | | | | | | 0.04 |
| 10 | | | | | | | 9.02 |
| 11 | | | | | | 15.14 | 0.49 |
| 12 | | | | | | 0.20 | 20.35 |
| 13 | | | | | | | 0 |
| 14 | | | 0 | 33.84 | 91.61 | 101.99 | 110.20 |
| 15 | | | | | | 29.04 | 50.52 |
| 16 | | | | | | | 0.01 |
| 17 | | | | 640.32 | 0 | 2.76 | 495.50 |
| 18 | | | | | 492.33 | 491.96 | 10.65 |
| 19 | | | | 179.12 | 492.33 | 435.42 | 382.06 |
| 20 | | | 694.12 | 10.44 | 0 | 0.89 | 0 |
| 21 | | | | | 0 | 0.01 | 0.08 |
| 22 | | | 6.24 | 0 | 13.70 | 12.40 | 11.50 |
| 23 | | | | 9.92 | 0 | 0.14 | 0.42 |
| 24 | | | 8.14 | 8.02 | 0 | 0.39 | 0.66 |
| 25 | | | 2.54 | 0 | 0 | 0.03 | 0 |
| 26 | | 228.01 | 1148.40 | 388.23 | 794.79 | 759.38 | 722.11 |
| 27 | | 228.01 | 147.72 | 1126.82 | 794.79 | 782.11 | 776.09 |
| 28 | | 0 | 34.44 | 28.21 | 0 | 1.12 | 2.12 |
| 29 | | | 103.91 | 118.50 | 103.88 | 95.99 | 88.95 |
| 30 | | | | 41.21 | 103.88 | 102.05 | 100.57 |
| 31 | | | | | 0 | 0.39 | 0.47 |
| 32 | | | | | | 4.34 | 5.95 |
| 33 | 104.70 | | | | | | 2.08 |

TABLE IX. Infrared intensities (in km/mol) for $H_2$ and the $H_{2n+1}^+$ ($n = 1$–4) at the TZP CISD level of theory.

| | $H_2$ | $H_3^+$ | $H_5^+$ | $H_7^+$ | $H_9^+$ |
|---|---|---|---|---|---|
| 1 | | | | | 0 |
| 2 | | | | | 0 |
| 3 | | | | 0 | 0 |
| 4 | | | | | 2.34 |
| 5 | | | | 10.10 | 2.33 |
| 6 | | | 0 | 24.05 | 72.77 |
| 7 | | | | | 618.81 |
| 8 | | | | 898.32 | 618.81 |
| 9 | | | 1816.04 | 205.47 | 0 |
| 10 | | | | | 0 |
| 11 | | | | 10.84 | 0 |
| 12 | | | | 0 | 15.20 |
| 13 | | | 7.06 | 7.97 | 0 |
| 14 | | | 11.16 | 13.47 | 0 |
| 15 | | | 6.13 | 0 | 0 |
| 16 | | 189.95 | 956.31 | 383.24 | 871.60 |
| 17 | | 189.95 | 73.69 | 1344.83 | 871.64 |
| 18 | | 0 | 82.89 | 25.76 | 0 |
| 19 | | | | | 104.02 |
| 20 | | | | 115.06 | 104.02 |
| 21 | 0 | | 97.69 | 41.51 | 0 |

($n = 3$–6), the results of Table VII are particularly pertinent. The fundamentals $\nu(A_1)$ (H–H) observed by OYL at 3910, 3980, 4020, 4028, and 4035 $cm^{-1}$ for $H_5^+$, $H_7^+$, $H_9^+$, $H_{11}^+$, and $H_{13}^+$, respectively, are predicted to have moderate intensities 103.90; 41.23 and 118.52; 0 and 104.87 (degenerate); 0.39 and 102.05; 0.47 and 100.57 km/mol, respectively, at the SCF level. Turning to CISD calculations until $n = 9$, the IR are predicted at 97.69; 41.51 and 115.06; 0 and 104.02 km/mol (degenerate) for $H_5^+$, $H_7^+$, and $H_9^+$, respectively, values not far from SCF predictions. Furthermore, concerning the highest frequencies of $H_{11}^+$ and $H_{13}^+$, they are predicted to have low intensities 4.34, 5.95, and 2.08, respectively. Among the normal modes that might be assigned to H–H stretching, the following modes 2377 ($n = 5$), 2693 ($n = 7$), 2656 (degenerate) ($n = 9$), 2671 ($n = 11$), and 2684 ($n = 13$) $cm^{-1}$ have by far the greatest predicted IR intensities 1148.40 ($n = 5$), 1126.80 ($n = 7$), 794.79 ($n = 9$), 782.11 ($n = 11$), and 776.09 ($n = 13$) km/mol, respectively, at the SCF level. The same trend is seen at the CISD level (Table IX).

As in the YGRS work, a strong dependence on the effects of electron correlation for the IR intensity is observed for the lower modes. Specifically, going from TZP SCF to TZP CISD, the intensity of the normal mode predicted at 511 $cm^{-1}$ (CISD) for $H_5^+$ increases from 694.10 to 1816.02 km/mol; the mode at 411 $cm^{-1}$ (CISD) for $H_7^+$ exhibits a smaller increase of intensity from 640.32 to 898.32 km/mol the intensity of the 444 $cm^{-1}$ mode (CISD) for $H_9^+$ increases from 492.33 to 618.81 km/mol. Nevertheless, although such predictions are quite sensitive to the level of theory employed, concerning the highest frequencies of each cluster, the IR intensities are relatively well predicted. Turning to the YGRS results at the SZP CISD level on $H_5^+$, our TZP CISD predictions differ from their own predictions by less than 15%.


[1] O. A. Schaeffer and S. O. Thompson, Radiat. Res. **10**, 671 (1959); W. D. Jones and W. T. Simpson, J. Chem. Phys. **32**, 1747 (1960); G. B. Pfeiffer, N. T. Huff, E. M. Greenalwaly, and F. O. Ellison, *ibid.* **46**, 824 (1967); J. T. J. Huang, M. E, Schwartz, and G. V. Pfeiffer, *ibid.* **56**, 755 (1972); R. D. Poshusta and F. A. Matsen, *ibid.* **47**, 4795 (1967); R. D. Poshusta J. A. Haugen, and D. F. Zetik, *ibid.* **51**, 3343 (1969); W. I. Salmon and R. D. Poshusta *ibid.* **59**, 4867 (1973); J. Easterfield and J. W. Linnett, J. Chem. Soc. Chem. Commun. 1970; 64; I. G. Kaplan and O. B. Rodimova, Intern. J. Quantum Chem. **5**, 669 (1971); S. W. Harrison, L. J. Massa, and P. Solomon, Chem. Phys. Lett. **16**, 57 (1972); Nature **245**, 31 (1977); K. G. Spears, J. Chem. Phys. **57**, 1850 (1972); R. Ahlrichs, Theor. Chim. Acta **39**, 149 (1975); D. Hyatt, P. N. Careless, and L. Stanton, Int. J. Mass Spectrom. Ion Phys. **23**, 45 (1977).

[2] S. Yamabe, K. Hirao, and K. Kitaura, Chem. Phys. Lett. **56**, 546 (1978); K. Hirao and S. Yamabe, Chem. Phys. **80**, 237 (1983).

[3] H. Huber, Chem. Phys. Lett. **70**, 353 (1980); H. Huber and D. Szekely, Theor. Chim. Acta **62**, 499 (1983); H. Huber, J. Mol. Struct. **121**, 287 (1985).

[4] S. Raynor and D. R. Herschbach, J. Phys. Chem. **87**, 289 (1983).

[5] Y. Yamaguchi, J. F. Gaw, and H. F. Schaefer III, J. Chem. Phys. **78**, 4047 (1983); Y. Yamaguchi, J. F. Gaw, R. B. Remington, and H. F. Schaefer III, *ibid.* **86**, 5072 (1987).

[6] M. Farizon, B. Farizon-Mazuy, N. V. de Castro Faria, and H. Chermette, Chem. Phys. Lett. **177**, 451 (1991).

[7] K. Buckheit and W. Henkes, Z. Angew. Phys. **24**, 191 (1968).

[8] R. Clampit and L. Gowland, Nature **223**, 815 (1968).

[9] N. A. Kulazhenkova, I. K. Larin, and V. L. Talroze, Dokl. Phys. Chem. **207**, 915 (1972).

[10] J. J. Thomson, Philos. Mag. **24**, 209 (1912); P. H. Dawson and A. W. Tickner, J. Chem. Phys. **37**, 672 (1962); A. Van Deursen and J. Reuss, Int. J. Mass Spectrom. Ion Phys. **11**, 483 (1973); A. Van Lumig and J. Reuss, *ibid.* **27**, 197 (1978); N. J. Kirchner and M. T. Bowers, J. Chem. Phys. **86**, 1301 (1987).

[11] U. A. Arifov, S. L. Pozhavov, I. G. Chernov, and Z. A. Mukhamediev, High Energy Chem. (USSR) **5**, 69 (1971).

[12] S. L. Bennet and F. H. Field, J. Am. Chem. Soc. **94**, 8669 (1972); M. T. Elford and H. B. Milloy, Aust. J. Phys. **27**, 795 (1974). M. T. Elford, J. Chem. Phys. **79**, 59 (1983); R. Johnsen, C. M. Huang, and M. A. Biondi, J. Chem. Phys. **65**, 1539 (1976); R. J. Beulher, S. Ehrenson, and L. Friedman, *ibid.* **79**, 5982 (1983).

[13] K. Hiraoka and P. Kebarle, J. Chem. Phys. **62**, 2267 (1975); K. Hiraoka, *ibid.* **87**, 4048 (1987); K. Hiraoka and T. Mori, Chem. Phys. Lett. **157**, 467 (1989).

[14] T. Oka, Phys. Rev. Lett. **45**, 531 (1980).

[15] M. Okumura, L. I. Yeh, and Y. T. Lee, J. Chem. Phys. **83**, 3705 (1985); **88**, 79 (1988).

[16] M. Chevallier, A. Clouvas, H. J. Frishkorn, M. J. Gaillard, J. C. Poizat, and J. Remillieux, Z. Phys. D **2**, 87 (1986); B. Mazuy, A. Belkacem, M. Chevallier, M. J. Gaillard, J. C. Poizat, and J. Remillieux, Nucl. Instrum. Methods B **28**, 497 (1987); M. Farizon, thesis, Lyon, 1988 (unpublished), M. Farizon, A. Clouvas, N. V. de Castro Faria, A. Denis, J. Desesquelles, B. Farizon-Mazuy, M. J. Gaillard, E. Gerlic, and Y. Ouerdane, Phys. Rev. A **43**, 121 (1991).

[17] K. P. Huber and G. Herzberg, *Constants of Diatomic Molecules* (Van Nostrand–Reinhold, New York, 1979).